

---

# Metallicity structure in X-ray bright galaxy groups

Jesper Rasmussen and Trevor J. Ponman

School of Physics and Astronomy, University of Birmingham, Edgbaston,  
Birmingham B15 2TT, UK [jesper@star.sr.bham.ac.uk](mailto:jesper@star.sr.bham.ac.uk)

**Summary.** Using *Chandra* X-ray data of a sample of 15 X-ray bright galaxy groups, we present preliminary results of a coherent study of the radial distribution of metal abundances in the hot gas in groups. The iron content in group outskirts is found to be lower than in clusters by a factor of  $\sim 2$ , despite showing mean levels in the central regions comparable to those of clusters. The abundance profiles are used to constrain the contribution from supernovae type Ia and II to the chemical enrichment and thermal energy of the intragroup medium at different group radii. The results suggest a scenario in which a substantial fraction of the chemical enrichment of groups took place in filaments prior to group collapse.

## 1 Introduction

Hot X-ray emitting gas constitutes the dominant baryonic component in groups and clusters of galaxies. The chemical enrichment of this intracluster medium (ICM) is believed to originate mainly in material ejected from group and cluster galaxies by supernovae, with a smaller portion driven out by galaxies through galaxy–galaxy and galaxy–ICM interactions. The spatial distribution of metals reflect the action of such processes, providing insight into the mechanisms, other than gravity, that have shaped the thermodynamic properties of gas in groups and clusters.

Iron and silicon comprise the major diagnostic elements for studies of the abundance distribution in groups and clusters, as these elements give rise to the most prominent lines in the soft X-ray spectrum of thermal plasmas, and are among the elements for which there is a distinctively different yield in type Ia and type II supernova explosions according to standard supernova (SN) models. Whilst iron is predominantly produced by SN Ia, silicon is more evenly mixed between the two SN types. The ratio of Si to Fe abundance therefore provides valuable information on the relative importance of SN II vs. SN Ia in enriching the intragroup medium.

Abundance profiles of massive clusters have received considerable attention. Due to their lower X-ray luminosities, the situation in lower-mass systems

is much less clear, despite their relatively larger importance for the cosmic baryon and metal budgets. With the current generation of X-ray telescopes, however, the ability to perform spatially resolved X-ray spectroscopy has improved dramatically, enabling detailed mapping of the metal distribution also in groups. Here we utilize this to derive radial profiles of the abundance of Fe and Si from *Chandra* observations of a sample of 15 groups. The sample size allows us to explore statistical trends within the sample and obtain a clearer picture of the content and behaviour of metals in group outskirts, where most of the intragroup gas resides but where the low X-ray surface brightness often prohibits robust constraints to be obtained for individual systems.

## 2 Sample and Analysis

Our sample is based on the 25 GEMS groups that show group-scale extended X-ray emission (the 'G' sample of [1]). Only groups with *Chandra* archival data featuring more than 6,000 net counts and being more distant than 20 Mpc were selected, while at the same time discarding obviously unrelaxed groups. We added four more groups conforming to these criteria, leaving a sample of 15 reasonably relaxed groups with high-quality *Chandra* data.

All data sets were subjected to standard screening criteria and cleaned for periods of high background, with blank-sky background data filtered in an identical manner. Background-subtracted spectra were extracted in annuli and fitted with a VAPEC model in XSPEC using Solar abundances from [2]. All elements were tied together, except for Fe and Si. To put all groups on an equal footing, all radii were normalized to  $r_{500}$ , the radius enclosing a mean density of 500 times the critical density, using an empirical relation based on the temperature of the group [3]. The temperature profiles themselves reveal that most of the groups feature a central region of cool gas, referred to here as the group core. For each group, Table 1 lists  $r_{500}$  and the mean temperature and abundance derived outside the cool core in the radial range  $0.1-0.3r_{500}$ .

**Table 1.** Basic X-ray properties of the group sample, with mean temperatures  $\langle T \rangle$  in keV, abundances  $\langle Z \rangle$  in  $Z_{\odot}$ , and  $r_{500}$  in kpc

Group	$\langle T \rangle$	$\langle Z \rangle$	$r_{500}$	Group	$\langle T \rangle$	$\langle Z \rangle$	$r_{500}$
NGC 383	$1.65^{+0.04}_{-0.06}$	$0.39^{+0.07}_{-0.07}$	578	NGC 4125	$0.33^{+0.12}_{-0.05}$	$0.19^{+0.17}_{-0.07}$	259
NGC 507	$1.30^{+0.03}_{-0.03}$	$0.40^{+0.07}_{-0.06}$	513	NGC 4325	$0.99^{+0.02}_{-0.02}$	$0.39^{+0.08}_{-0.06}$	448
NGC 533	$1.22^{+0.05}_{-0.05}$	$0.28^{+0.07}_{-0.06}$	497	HCG 62	$1.00^{+0.03}_{-0.03}$	$0.12^{+0.02}_{-0.03}$	450
NGC 741	$1.42^{+0.14}_{-0.12}$	$0.16^{+0.08}_{-0.06}$	536	NGC 5044	$1.12^{+0.03}_{-0.03}$	$0.25^{+0.04}_{-0.03}$	476
NGC 1407	$1.01^{+0.07}_{-0.09}$	$0.15^{+0.09}_{-0.06}$	452	NGC 5846	$0.66^{+0.04}_{-0.03}$	$0.16^{+0.06}_{-0.05}$	366
NGC 2300	$0.78^{+0.04}_{-0.03}$	$0.17^{+0.07}_{-0.05}$	397	NGC 6338	$2.13^{+0.19}_{-0.07}$	$0.25^{+0.08}_{-0.05}$	657
HCG 42	$0.80^{+0.05}_{-0.05}$	$0.25^{+0.31}_{-0.10}$	402	NGC 7619	$1.06^{+0.07}_{-0.03}$	$0.23^{+0.05}_{-0.05}$	463
NGC 4073	$1.78^{+0.07}_{-0.09}$	$0.49^{+0.07}_{-0.07}$	600				

### 3 Fe and Si Radial Profiles

Profiles of Fe and Si abundance for all groups combined are shown in Fig. 1a. Fe is seen to decline outside the group core, converging towards a value of  $\sim 0.1 Z_{\odot}$  at  $r_{500}$ . We note that this value is lower than that seen in cluster outskirts by a factor of  $\sim 2$  (e.g. [4]), even though the Fe abundance in group cores is comparable to cluster levels. Si is more spatially uniform than Fe, declining less steeply outside the core. Intrinsic scatter is most prominent in the core, where non-gravitational processes are expected to be important.

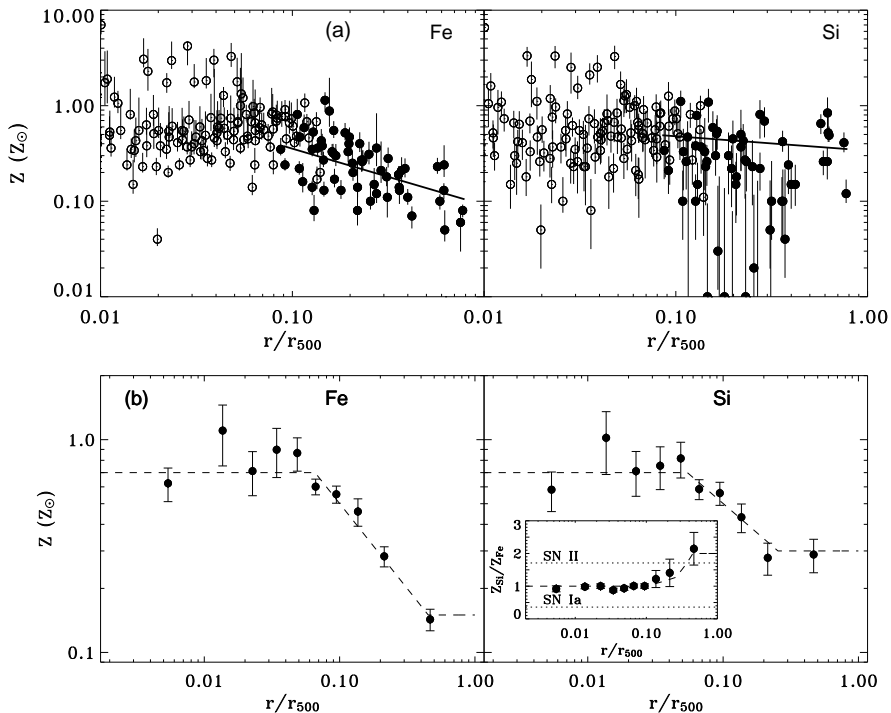


**Fig. 1.** (a) Radial abundance profiles for all groups. Filled circles represent data points outside the cool group cores, empty circles those within. Solid lines represent the results of regression fits to the data outside the group cores. (b) The same data, binned into radial bins of 20 data points. The inset shows the resulting Si/Fe ratio, with dotted lines marking the expectations from pure SN Ia and SN II enrichment

These features are all confirmed by Fig. 1b, where the data have been binned into radial bins of 20 measurements, to help illustrate any radial trends. Adopting the SN model yields of [5, 6], the Si/Fe ratios suggest that the enrichment in group cores can be attributed to a mixture of SN Ia and SN II which is similar to that in the Solar neighbourhood. At large radii the Si/Fe

ratio suggests an increasing predominance of SN II, with the abundance pattern being consistent with pure SN II enrichment at  $r_{500}$ .

As the intrinsic scatter in abundances outside the group cores is fairly small, we made simple parametrizations of the binned profiles shown in Fig. 1b, in order to obtain prescriptions for  $Z_{\text{Fe}}(r)$  and  $Z_{\text{Si}}(r)$  that can be seen as representative for the entire group sample. These are shown as dashed lines in Fig. 1b, with the resulting (parametrized) ratio  $Z_{\text{Si}}(r)/Z_{\text{Fe}}(r)$  conforming to the range allowed by the adopted SN yields.

## 4 Implications

### 4.1 Metal Masses and the Role of SN Ia vs. SN II

Based on gas density profiles for each group taken from the literature, the parametrized Fe and Si profiles were decomposed into contributions from SN Ia and SN II. The result, shown in Fig. 2a, indicates that about half of the iron in group cores is provided by SN Ia, but that SN II products are much more widely distributed than those of SN Ia, similarly to results for clusters. The total iron mass released by SN within  $r_{500}$  spans the range  $3 \times 10^7 - 3 \times 10^9 M_{\odot}$  across the sample.

Using optical luminosities derived as in [1], total iron mass-to-light ratios within  $r_{500}$  are shown in Fig. 2b (results for Si are very similar). The low Fe abundance in group outskirts compared to clusters is reflected in lower Fe  $M/L$  ratios. Even across the fairly narrow range in total group mass studied here (estimated assuming an empirical mass-temperature relation  $M \propto \langle T \rangle^{1.5}$  [7]), there is a clear tendency for lower-mass groups to contain relatively lower amounts of enriched material for their optical luminosity.

Assuming each SN releases  $10^{51}$  erg directly into the ICM, the total SN energy range displayed by the groups of  $2 \times 10^{59} - 2 \times 10^{61}$  erg is comparable to the total thermal energy contained in the ICM, with the clear majority of it ( $\sim 95\%$ ) provided by SN II.

### 4.2 The Chemical Enrichment History of Groups

Figures 1 and 2 show that the metals are not completely mixed throughout the ICM. This applies particularly to the metals attributed to SN Ia, of which a considerable fraction is likely to be associated with prolonged enrichment from the stellar population of the central galaxy present in all the groups. As also discussed by [4] on the basis of a small sample of three groups, the much wider distribution of SN II products suggests a scenario of SN II-dominated enrichment at an early stage in the formation of the groups, leaving time for the enriched material to mix well throughout the ICM.

In the group outskirts, the inferred energy per particle imparted to the IGM by SN II is of order 0.5 keV. Coupled with the above, this indicates

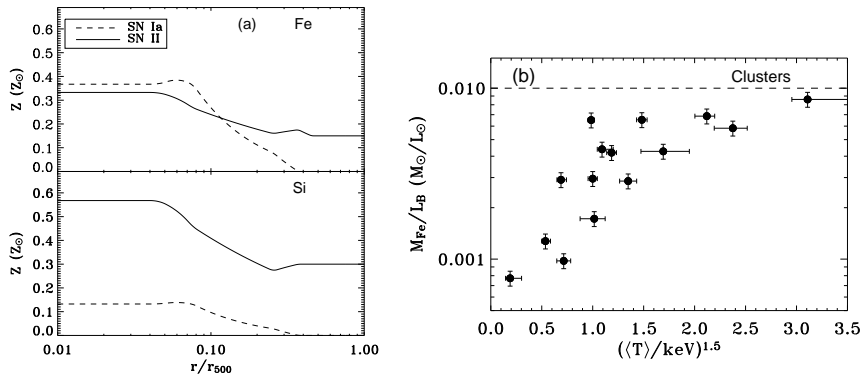


**Fig. 2.** (a) Contribution to the total abundance of Fe and Si from SN Ia and SN II. (b) Fe mass-to-light ratio within  $r_{500}$  as a function of group mass'  $M \propto \langle T \rangle^{1.5}$ . The dashed line shows the typical cluster value [4]

that galactic winds associated with an early phase of strong starburst activity could have contributed substantially to pre-heating of the ICM in groups. It is likely that much of this preheating and the associated chemical enrichment took place before the gas collapsed into groups, while still located in filaments of low overdensities [8]. Some fraction of the SN ejecta should have been able to escape from low-mass filaments, giving rise to the trend of increasing iron mass-to-light ratio with present-day group mass. The inferred central rise in SN II products can then be explained if some of these metals were released after the group collapsed, possibly facilitated by galaxy–galaxy and galaxy–ICM interactions, and potentially with an additional contribution associated with stellar wind loss from the central elliptical galaxy.

We are grateful to Stephen Helsdon for his contribution to the early stages of this work. JR acknowledges the support of an EU Marie Curie Intra-European Fellowship under contract no. MEIF-CT-2005-011171.

## References

1. J.P.F. Osmond, T.J. Ponman: MNRAS **350**, 1511 (2004)
2. N. Grevesse, A.J. Sauval: Space Sci. Rev. **85**, 161 (1998)
3. A. Finoguenov, T.H. Reiprich, H. Böhringer: A&A **368**, 749 (2001)
4. A. Finoguenov, L.P. David, T.J. Ponman: ApJ **544**, 188 (2000)
5. K. Nomoto, et al.: Nucl. Phys. A **616**, 79 (1997)
6. K. Nomoto, et al.: Nucl. Phys. A **621**, 467 (1997)
7. A. Vikhlinin, A. Kravtsov, W. Forman, C. Jones, M. Markevitch, S.S. Murray, L. Van Speybroeck: ApJ submitted (astro-ph/0507092)
8. T.J. Ponman, D.B. Cannon, J.F. Navarro: Nature **397**, 135 (1999)